Production of H_2 from ethanol using bimetallic Ni-Co/hydrotalcite catalysts promoted with WOx

A. Figueroa[1], J.L.Contreras[1,*], L. Nuño-Licona[1],G. Fuentes2, B. Zeifert[3] , J. Salmones[3], T. Váquez[4],B. Quintana-Díaz[1] y C. Tapia-Medina[1]

[1]Universidad Autónoma Metropolitana-Azcapotzalco, CBI-Energía, Av. Sn. Pablo 180,,
Col. Reynosa, C.P. 02200, México D.F., México.
[2]Universidad Autónoma Metropolitana-Iztapalapa,CBI- Depto. de IPH, A.P.55-534, 09340,México, D.F.
[3]Instituto Politécnico Nacional, ESIQIE, Unidad Prof. ALM, México, D. F., 07738, México
[*]Tel: 53189065 Ext 116, mail: jlcl@correo.azc.uam.mx

ABSTRACT

Ni-Co/Hydrotalcite-WOx catalysts were active in the ethanol steam reforming producing H_2, CH_3CHO, CO_2, CH_4 and $CH_2=CH_2$. The Ni and Co amount in the bimetallic catalysts did not change the selectivity observed respect to the selectivity of the monometallic catalysts. The bimetallic catalysts of Ni-Co showed higher conversions than the conversion of the monometallic Ni catalyst. The surface area in the Ni and Co catalysts was nearly inversely proportional to the metal concentration. Metal oxides of Ni and Co in the bimetallic catalysts interacted with the hydrotalcite structure, causing a partial blockage of pores, resulting in a decrease of pore volume. By XRD diffraction analysis we observed a laminar structure typical of hydrotalcites and the absence of NiO and CoO phases suggested that probably both Ni^{2+} and Co^{2+} have isomorphically replaced the Mg^{2+} cations in the hydrotalcite structure. The infrared results suggested that some of the –OH groups in the brucite type layers of the hydrotalcite could be substituted by Ni and Co oxo-species. The Ni-Co bimetallic catalyst with 2%Co showed the highest conversion and also the highest production to H_2.

1. Introduction

Ethanol has several advantages as a fuel, for example it can be more easily stored without significant handling risk and it can be obtained in large quantities from biomass [1-2]. An energy balance has shown that approximately 35% of the total energy obtained by hydrogen combustion is required to produce hydrogen, whereas the remaining 65% is the available energy [3]. Then in order to produce H_2 using catalysts by ethanol steam reforming, they must show high thermal stability, because the relative high operation temperatures at which reforming reactions take place, as well as high selectivity to the H_2 production and also avoiding the formation of undesired products such as: acetaldehyde, diethyl ether, acetic acid and ethylene.

The influence of the nature the active sites and the environment of these sites on catalyst performance has been important [4]. The design of these active sites has been a key requirement to develop supported catalysts that fulfill the above requirements.

The catalytic properties of supported transition metals of the groups VIII, IX and X for hydrogen production from ethanol steam reforming have already been investigated in the last years [5,4]. The studies concluded that several supported noble metals such as Ir, Pt, Pd, Ru or Rh [6,7], or inexpensive metals such as Co [8-10], Ni [11,10,12], Cu [13] or bimetallic materials [13-15] are good options to catalyze the ethanol steam reforming. Thereby, supports such as: MgO, ZnO, SiO_2, Al_2O_3, La_2O_3 or CeO_2, among others, are the most commonly used to support the active metals [11,8,16].

The activity and hydrogen selectivity depends on the properties of the active metal, the support of the active metal and the conditions of the reaction, among other variables. Accordingly with López et al.[17], the non-expensive active metals and supports with non-acid character are considered the best option due to: (i), the delay of coke deposition, decreasing the surface poisoning [7,8,16,18]; and (ii), the promotion of the dehydrogenation of ethanol to acetaldehyde reaction [9]. On the other hand, the stabilization of active metals can allow increasing the reaction temperature and at the same time: (j), it avoids metal sintering, and (jj), increases the hydrogen selectivity. Thus, the incorporation of the active metals into a mixed oxide matrix may be a strategy to stabilize the metal active centre. Other option is to deposit the active metals on a stabilized support for example with tungsten oxides [11].

Other kind of mixed oxides able to stabilize metals into their structure includes the oxides derived from the so-called hydrotalcite-like compounds, also known as layered double hydroxides (LDHs) [19]. LDHs are a family of lamellar materials derived from brucite layers, which are currently of intense academic and industrial interest [19-22]. These compounds contain M^{2+} and M^{3+} metal cations. These cations are capable of occupying the octahedral interstices of a brucite-like sheet by partial substitution of magnesium. Also, there are exchange anions positioned in the gallery between the layers in order to balance the positive charge of the layers [19]. Upon heating, these highly ordered LDHs form an amorphous mixture of metal oxides-$M^{2+}M^{3+}(O)^{-}$ with small crystal size and high thermal stability named as ex-LDH. These ex-LDH systems have shown interesting properties, such as high dispersion of the active metals, high specific surface areas [23,19,24], high interaction between different cations in the oxide matrix [25], “memory effect” [19] or controllable acid/basic character [19,22], which can control coke deposition in the EtOH reforming reaction [26].

The aim of this study is to know the catalytic activity and selectivity of bimetallic Ni-Co/hydrotalcite-WOx catalysts. The WOx compounds stabilized the hydrotalcite support in a similar way than any other metal cation. The Ni and Co metals were impregnated, calcined and reduced on the hydrotalcite-WOx support.

2. Experimental

2.1.-Catalysts Preparation

The hydrotalcite was made by coprecipitation using two salt solutions as precursors. First, in a stirred reactor a salt solution of $Mg(NO_3)_2$ and $Al_2(NO_2)_3$ (J.T. Baker) with a molar ratio of 2:1 was made. A second solution of Na_2CO_3 (5%) and NaOH (pH = 10) (Carlo Erba) was prepared. These two solutions were added simultaneously drop

by drop to a third stirred reactor using water as solvent (60 drops/min) at 60°C maintaining an atomic ratio of Mg^{2+}/Al^{3+} of 1.55. In this step a solution of $(NH_4)_{12}W_{12}O_{41}\bullet 5H_2O$, (Aldrich) was added in order to get %wtW of the final solid. After aging the precipitate for 24 h the resulting solid was washed, dried and calcined at 450°C for 5h (sample HT). A solution of $Ni(NO_3)_2$ was impregnated in such a way as to get a constant amount of 1 wt% Ni (sample HTN), In the case of the Co catalyst, a solution of $Co(NO_3)_2$ was impregnated in such a way as to get a constant amount of 1 wt% Co (sample HTC). The bimetallic samples were: 1wt%Ni-2wt%Co (N1C2), 2wt%Ni-1wt%Co (N2C1). The impregnation of the solids was made during 2 h at 60°C. The solids were washed, dried at 120°C for 24 h and calcined at 450°C during 5 h. Finally the samples were reduced with pure H_2 at 500°C for 2 h.

2.2.- Catalysts Characterization

The solids obtained were characterized by X-ray diffraction (XRD) in a Phillips X´ Pert instrument. The XRD patterns of the samples after calcination were obtained using the CuKα radiation. Diffraction intensity was measured in the 2θ range between 5 and 70° with a 2θ step of 0.02° with 8 seconds per point, the samples were analyzed directly at room temperature. The infrared spectroscopy was made in a Perkin Elmer spectrophotometer (Spectrum-RX). An infrared beam was sent through a wafer of the sample. The wavenumber range was from 4000 to 400 cm^{-1} and the number of scans averaged was 50. N_2 physisorption at 77 K was made in a Micromeritics 2000 instrument. Each sample was pretreated at 200°C under vacuum (1 x 10^{-4} torr).

2.3.- Catalytic evaluation for steam reforming of ethanol.

The catalytic reaction was made in a U-shaped stainless steel fixed bed reactor. The catalyst (1g) was charged for each of the reaction evaluation. The feed of the reactants consisted of ethanol (Aldrich), water as steam and N_2 (purity 99.99%, Infra-Air Products). N_2 was fed through a micrometric needle valve (1 ml/s). The gas mixture of H_2O and CH_3CH_2OH (molar ratio of 4/1) in N_2 stream was prepared using two glass saturators followed by heating to 92°C before it should be feed to the reaction chamber.

The temperature of the catalyst was changed to 450°C in flow of N_2 for 30 min to clean the catalyst surface and then the flow of reactants started at 450°C. The catalyst was held at that temperature for 30 min in order to make three analyses. In the case of deactivation tests the catalysts were evaluated during 420 min.

The analysis of the reactants and all the reaction products was carried out online by gas chromatography. Inside an automated injection valve, the sample was divided into two portions which were then analyzed in order to obtain accurate, complete quantification of the reaction products. One sample was used to analyze H_2, CO, CO_2 and CH_4, using a column of silica gel 12 grade 60/80 (18´x 1/8") with a thermal conductivity detector (Gow-Mac apparatus). The second sample was used to analyze CH_3CH_2OH, CH_3CHO, CH_3COCH_3, CH_2O and $CH_2{=}CH_2$ with a capillary column (VF-1ms, 15m x 0.25 mm) in a Varian chromatograph CP-3380 with a flame ionization detector (FID). Response factors for all products were obtained and the system was calibrated with appropriate standards before each

catalytic test. The conversion (X) was calculated using the ethanol composition before and after of the reaction. The selectivity of each product was defined as follows: Si (%) = Ni / Σ Nj x 100 where: Si (%) = Selectivity to product i Ni = Moles of product i , Nj = Moles of each product (included i) .

3.- Results and discussion

3.1.- Textural properties

The surface area in the Ni and Co catalysts was nearly inversely proportional to the metal concentration (Table 1). The sample free of metals (sample HT) showed the widest pore distribution (50 to 1000 Å) having an average pore diameter of 539Å (Figure 1), while the monometallic samples with the Ni (HTN) and Co (HTC) showed a smaller average pore diameter of 250 Å for HTN sample and 469Å for HTC sample.

Table 1. Surface area BET and metal concentration of the Ni-Co/Hydrotalcite-WOx catalysts

Catalysts	Ni (wt%)	Co (wt%)	Surface area BET (m^2/g)	Pore volume by (cm^3/g)	Pore diameter (Å)
HT	0	0	220	0.21	539
HTN	1	0	216	0.15	250
HTC	0	1	213	0.16	248
N2C1	2	1	195	0.13	510
N1C2	1	2	188	0.12	498

In these two samples the metal oxides of Ni and Co interact with the hydrotalcite structure, causing a partial blockage of pores, resulting in a decrease of volume pore. Particularly, this phenomenon was already reported by Basile et al. [14] who suggested that such a decrease in the surface area was related to the aggregation of metallic species blocking the smaller pores and/or causing some structural rearrangements. Further addition of both metals (samples N2C1 N1C2) to the hydrotalcite produced samples with pore diameter between that obtained of the HT sample and the samples HTN. At small Ni concentrations there is pore blocking on the hydrotalcite interlayers, thus reducing the pore diameter. While at higher concentrations of Ni and Co could be a the collapse of some interlayers of the hydrotalcite structure and therefore producing lower pore volumes. Another possible explanation is that at low Ni concentrations (sample HTN) Ni may substitute some species in the hydrotalcite structure, causing a narrower interlayer structure and therefore lower pore volumes than in sample HT.

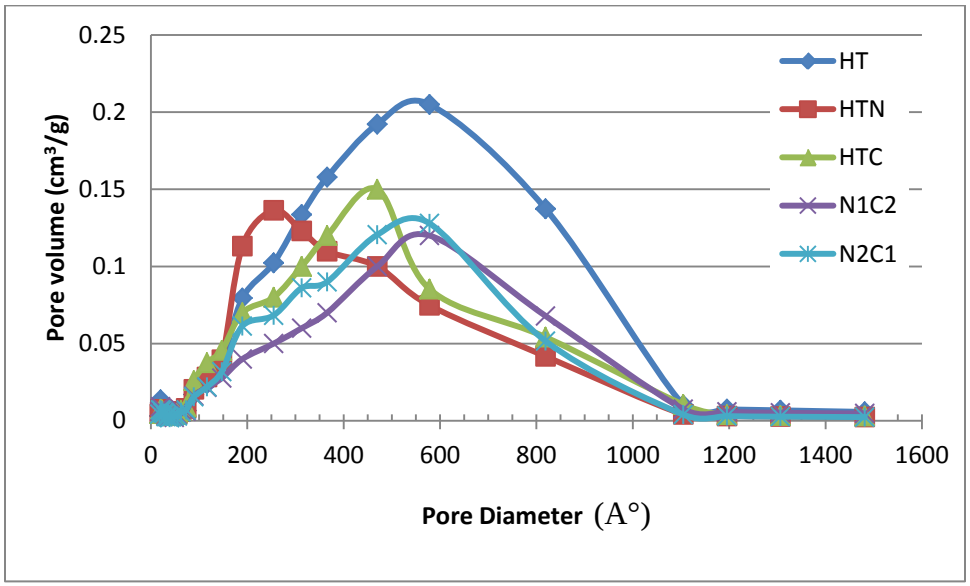

Figure 1. Pore diameter distribution of the Ni-Co/Hydrotalcite-WOx catalysts

3.2.- XRD analysis

For sample HT, XRD showed symmetric intense peaks corresponding to (003), (006), (110) and (113) reflections (Figure 2). Additionally, we observed asymmetric peaks with smaller intensity in (012), (015) and (018). These peaks correspond to a laminar structure typical of hydrotalcites [13].

At larger Ni and Co concentration the crystalline structure of the samples decreased. The absence of NiO and CoO phases suggests that both Ni^{2+} and Co^{2+} have isomorphically replaced the Mg^{2+} cations in the burcite ($Mg(OH)_2$) -like layers [23, 4,9,15]. The intensity of the diffraction lines assigned to the hydrotalcite phase decreased by the addition of these ions, suggesting a decrease in the population of Mg-Al-Hydrotalcite structures. The Ni^{+2} and Mg^{+2} exchange could be possible [16], but that is difficult to ascertain with the low Ni concentration used.

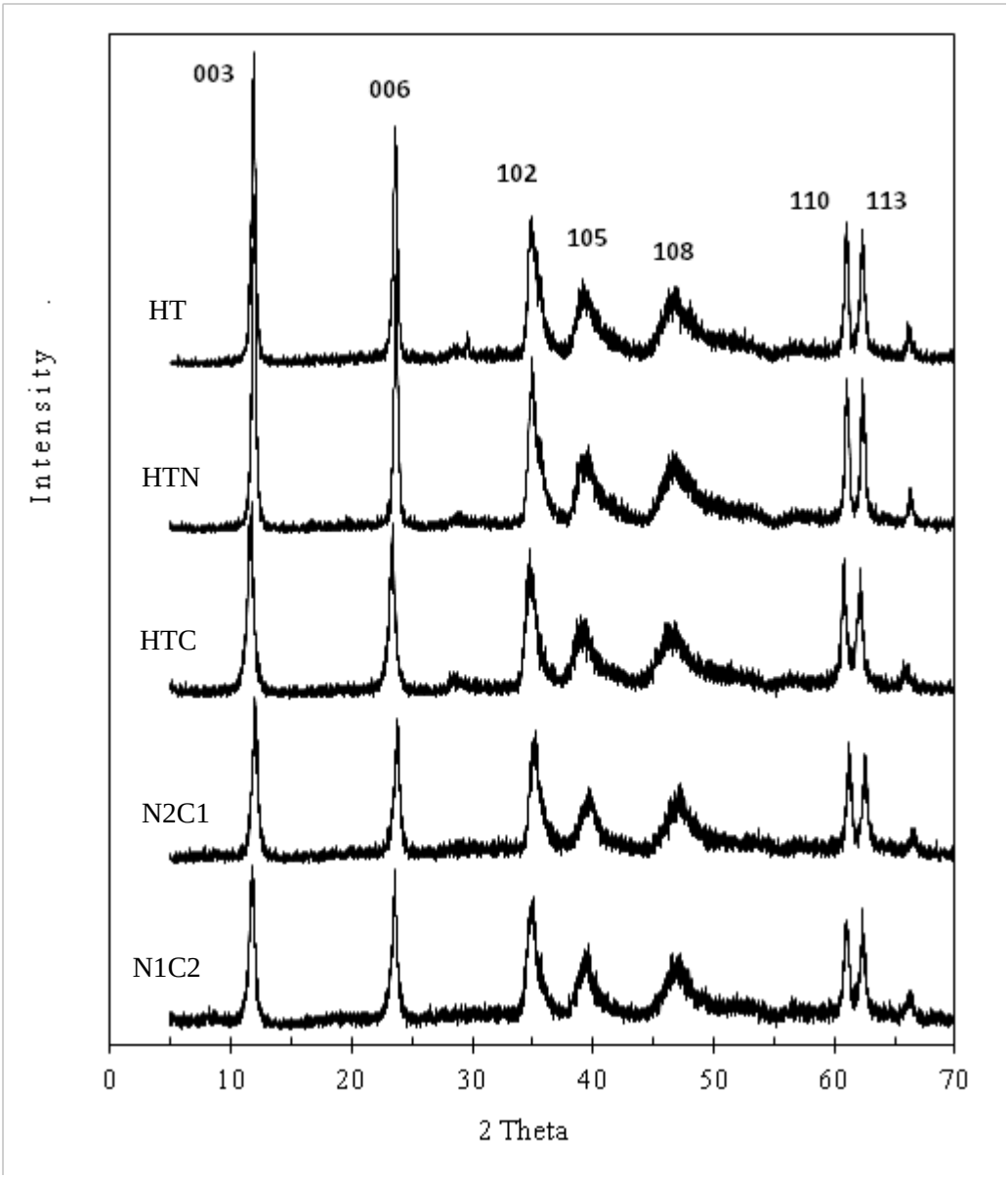

Figure 2. XRD of the monometallic and bimetallic Ni-Co/Hydrotalcite-WOx catalysts (calcined at 450°C)

3.3.- Infrared spectroscopy

The infrared spectra for the samples with Ni and Co (Figure 3) showed a broad OH stretching band in the 3100-3800 cm^{-1} region and the H_2O scissoring mode band near 1500-1600 cm^{-1} provides evidence for the presence of water molecules. Other authors have attributed the band at 3410 cm^{-1} to hydroxil groups coordinated with Mg and Al, while the vibration of the same group associated with water is a wide band between 3650-3590 cm^{-1} [18]. . The

lowest absorbance was for the catalyst HTC. This suggests that this catalyst had the lowest amount of hydroxil groups –OH.

A strong band located at 1380 cm^{-1} is attributed to the presence of residual nitrate ions. Another band located at 1029 cm^{-1} is related with the symmetric C=O stretching carbonate ion which has been found in 1041cm^{-1}[19]. In the region below 1000 cm^{-1} the spectrum showed a band located in 772 cm^{-1} assigned to –OH bending vibrations of brucite ($Mg(OH)_2$) type layers [20].

The bands located at 680 and 560 cm^{-1} correspond to vibration modes of brucite-type layers, specifically the metal-oxygen symmetrical stretching. The antisymmetric -OH stretching band located at 3460 cm^{-1} decreased as the Ni and Co concentration increased, and so did the H_2O scissoring mode band at 1600 cm^{-1}. These results suggest that some of the –OH groups in the brucite type layers of the hydrotalcite could be substituted by Ni and Co species.

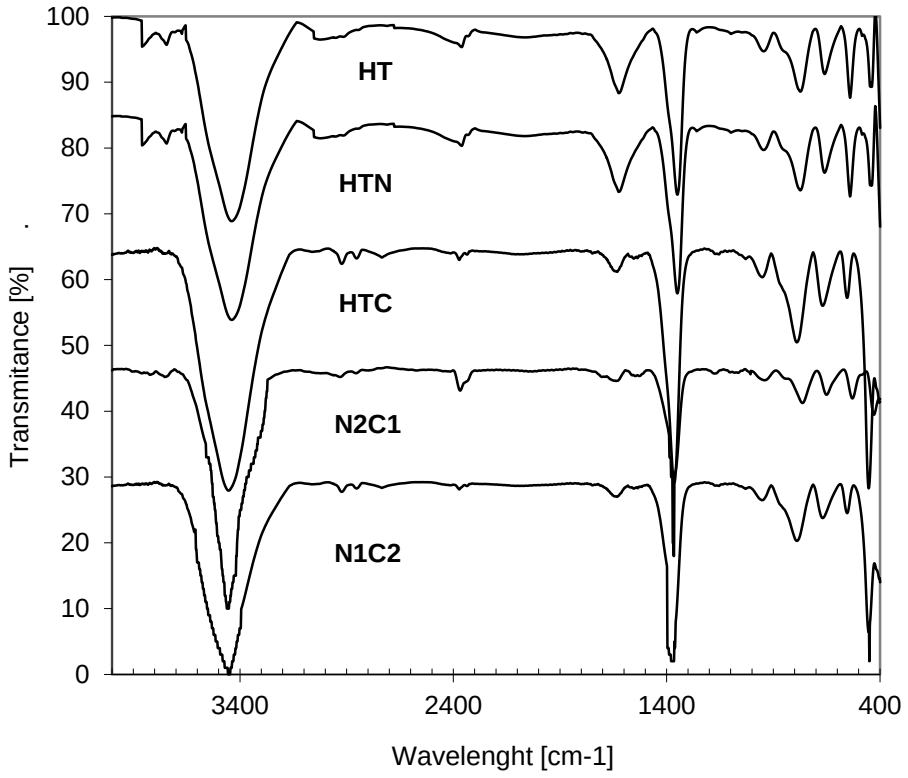

Figure 3. Infrared spectra of the monometallic and bimetallic Ni-Co/Hydrotalcite-WOx catalysts

3.4.- Catalytic activity

Ni-Co/Hydrotalcite catalysts were active in the ethanol steam reforming producing H_2, CH_3CHO, CO_2, CH_4 and $CH_2=CH_2$ (Figure 4). The Ni and Co amount in the bimetallic catalysts did not change the selectivity observed respect to the selectivity of the monometallic catalysts (HTN and HTC). For this type of catalysts, the production of ethylene, acetaldehyde and diethyl ether decreased as reaction temperature increased.

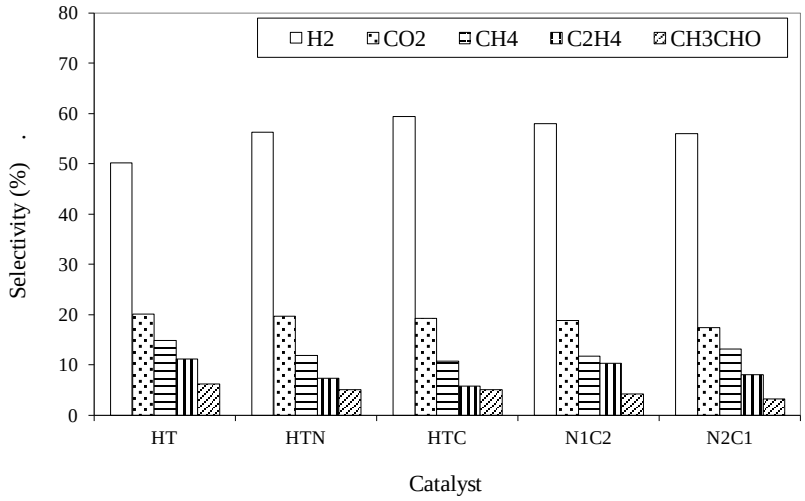

Figure 4. Selectivity of products from Ni-Co/Hydrotalcite-WOx catalysts evaluated at 450°C

The reaction products in Figure 4 are produced in accordance with the following reactions:

$CH_3CH_2OH + 3\,H_2O \rightarrow 2\,CO_2 + 6\,H_2$ (1)

$CH_3CH_2OH \rightarrow CH_3CHO + H_2$ (2)

$CH_3CH_2OH + H_2O \rightarrow CO_2 + CH_4 + 2\,H_2$ (3)

$CH_3CH_2OH \rightarrow CH_2=CH_2 + H_2O$ (4)

$CO + H_2O \rightarrow CO_2 + H_2$ (water-gas shift reaction) (5)

$CH_4 + H_2O \rightarrow CO + 3\,H_2$ (6)

$CH_2=CH_2 + 2\,H_2O \rightarrow CH_4 + CO_2 + 2\,H_2$ (7)

$CH_3CHO + H_2O \rightarrow CH_4 + CO_2 + 2\,H_2$ (8)

The presence of CH_3CHO was observed in all the catalysts studied, suggesting that Ni-Co/hydrotalcite surface acted as a dehydrogenation catalyst according to reaction (2) and H_2 was the main product with several reactions contributing to its production (mainly reaction 1). We did not detect CO perhaps because it reacted with water to produce CO_2 and more H_2 in accordance with reaction (5) or because reaction (1) was more favored than reactions

(3) and (6) which are the route for CO production. Although some CO can be produced at thermodynamic equilibrium it may not be relevant in continuous operation because the methane reforming reaction (6) is not favored at temperatures below 450°C and it is also kinetically limited. Therefore, the most relevant reactions describing results from Figure 4 are reactions (1), (2), (3) and (4).

The ethanol dehydration to CH_2=CH_2, reaction (4) was not dependent on both Ni and Co concentrations however it has been reported [18] that for Ni-hydrotalcite catalysts, the higher the Ni loading, the lower is the selectivity to ethylene and diethyl ether. Additionally, it is important to remember that the presence of these products could lead to the formation of coke [27], and their yield has a space-time dependence typical of intermediate products [28].

The difference in H_2 selectivity between all the catalysts was small and H_2 production comes from several reactions; dehydrogenation, water-gas shift conversion of CO and decomposition of oxygenated compounds. Infrared studies have shown that dehydrogenation of molecularly adsorbed ethanol was a key reaction step [29].

Ethanol adsorbs molecularly to form weakly adsorbed hydrogen-bonded species and to produce strongly adsorbed molecular ethanol on the Lewis-sites of the support. It was found that high temperature treatment of the adsorbed species caused the formation of surface acetate species on the support. The presence of water lowered the temperature for the appearance of acetate species and increased the stability of monodentate ethoxide species.

The N1C2 catalyst showed the highest conversion (Figure 5) and also the highest production to H_2. Bimetallic N2C1 catalyst showed less conversion than the monometallic Co catalyst (HTC).

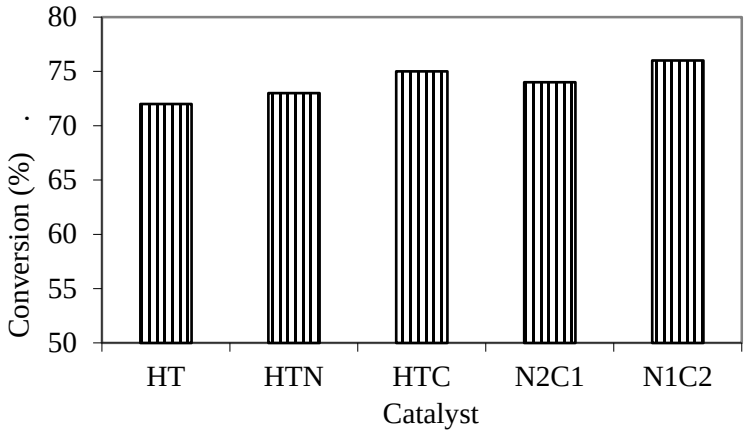

Figure 5. Catalytic conversion of the Ni-Co/hydrotalcite-WOx catalysts evaluated at 450°C.

Some authors have worked with catalysts containing hydrotalcites [30] or hydrotalcite-like compound precursors with different preparation methods to produce H_2. For example, Liu et al [31] prepared their solids by a novel method, which was a combination of the reverse microemulsion and coprecipitation methods. It was observed that the precursor obtained from the above method possessed superior characteristics for preparing mixed oxide catalyst

used in ethanol steam reforming. The authors mentioned that the reverse microemulsion-derived catalyst showed much better catalytic performance than catalysts prepared from conventional coprecipitation or impregnation methods in terms of H_2 selectivity and catalyst stability. However our precipitation method produced catalysts with equivalent stability during the deactivation test at 450°C. Other authors [32] prepared catalysts with Ni loaded Mg-Al mixed oxide supported catalysts which were superior in H_2 and COx product selectivity and stability compared to the pure oxide supported Ni catalysts. Recently, there are other authors using hydrotalcites or ex-hydrotalcites with other metals (La, Ce, Zn, Co, Cu) which cause a high stabilization of the active metal phases in similar way than W and with good selectivity to H_2 [33-36].

In relation with the chemical surface of these solids, the presence of surface –OH on the catalyst (infrared experiments) has been reported to be important to catalyze the initial interaction of ethanol with these –OH groups to form ethoxy species [37] which could evolve to produce CH_3CHO. This compound may evolve over the surface through alkyl elimination or by forming a bidentate acetate species, which through C-C scission can produce CO_2, CH_4 and H_2 in the presence of water. This explanation may be similar for the steam reforming of ethanol using ZnO in which this oxide has showed catalytic activity producing H_2, CO_2 and CH_3CHO [29].

4. Conclusions

The surface area in the Ni and Co catalysts was nearly inversely proportional to the metal concentration. Metal oxides of Ni and Co in the bimetallic catalysts interacted with the hydrotalcite structure, causing a partial blockage of pores, resulting in a decrease of pore volume. By XRD diffraction we observed a laminar structure typical of hydrotalcites and the absence of NiO and CoO phases suggested that probably both Ni^{2+} and Co^{2+} have isomorphically replaced the Mg^{2+} cations in the hydrotalcite structure. The infrared results suggested that some of the –OH groups in the brucite type layers of the hydrotalcite could be substituted by Ni and Co oxo-species.

Ni-Co/Hydrotalcite-WOx catalysts were active in the ethanol steam reforming producing H_2, CH_3CHO, CO_2, CH_4 and $CH_2=CH_2$. The Ni and Co amount in the bimetallic catalysts did not change the selectivity observed respect to the selectivity of the monometallic catalysts. The bimetallic catalysts of Ni-Co showed higher conversions than the conversion of the monometallic Ni catalyst. The Ni-Co bimetallic catalyst with 2%Co showed the highest conversion and also the highest production to H_2.

5. Acknowledgements

To the Universidad Autónoma Metropolitana-Azcapotzalco and Iztapalapa, to the Instituto Mexicano del Petróleo and the Instituto Politécnico Nacional- ESIQIE of México for their financial and academic support.

7. References

[1] R.D. Cortright, R.R. Davda, J.A. Dumesic, Nature 418, 964(2002).

[2] J. Llorca, N. Homs, J. Sales, J. L. G. Fierro and P. Ramírez de la Piscina, J. Catal. 222, 470-480(2004).

[3] M.A. Ortiz R., Hydrogen from bio-ethanol using Co, Ni and Pt hydrotalcites, stabilizated with WOx, Chem. Eng. Thesis UAM-Azcapotzalco, México (2009).

[4] J. L.Contreras, J. Salmones, L. A. García, A. Ponce, B. Zeifert and G.A. Fuentes, J. of New Materials for Electrochemical Systems 11, 109-117(2008).

[5] A. Aboudheir, A. Akande, R. Idem, A. Dalai, Int. J. of Hydrogen Energy 31,752-761(2006).

[6] H. Liandro Reza G., Síntesis y caracterización fisicoquímica de catalizadores sólidos básicos tipo hidrotalcita de cobalto y níquel. Tesis de licenciatura, Universidad Autónoma Metropolitana, Unidad Azcapotzalco (2003).

[7] M. N. Barroso, M. F. Gómez, L. A. Arrúa, M. C. Abello, Appl. Catal. A:General 304, 116-123(2006)

[8] J. Llorca, N. Homs, J. Sales, and P. Ramírez de la Piscina, J. Catal. 209, 306-317(2002).

[9] K. Sing, D. Everett, R. Haul, L. Moscou, R. Pierotti, J. Rouquerol, and T. Siemieniewska, Pure Appl. Chem. 57, 603 (1985).

[10] L. D. Gelb, K. E. Gubbins, R. Radhakrishnan, and M. Sliwinska-Bartkowiak, Reports on Progress in Physics 62, 1573 (1999).

[11] J. L .Contreras, G. A. Fuentes, J. Salmones, B. Zeifert, J. of Alloys and Compounds 483, 371-373(2008).

[12] S. Lowell, J. E. Shields, M. A. Thomas, and M. Thommes, Characterization of Porous Solid and Powders: Surface Area, Pore Size and Density, Kluwer Academic Publishers, (2004).

[13] M. del Arco, D. Carriazo, S. Gutiérrez, C. Martín and V. Rives, Inorg. Chem. 43, 375-384(2004).

[14] F. Basile, G. Fornasari, M. Gazzano, A. Vaccari, Appl. Clay. Sci. 16,185(2000).

[15] A.C.C. Rodríguez,C.A. Enríquez, J.L.F. Monteiro, Mater. Res. 6, 563(2003).

[16] T. Shishido, M. Sukenobu, H. Morioka, R. Furukawa, H.l Shirahase, K. Takehira, Catal. Lett.73, 21(2001).

[17] .G. López, R.M. Navarro, M.A. Peña, J.L.G. Fierro, Int. J. of Hydrogen Energy, 36,1512-1523(2011).

[18] María de los Ángeles Ocaña Zarceño, Síntesis de Hidrotalcitas y Materiales Derivados: Aplicaciones en Catálisis Básica. Tesis de Doctorado, Universidad Complutense de Madrid (2005).

[19] C. Resini, T. Montenari, L. Barattini, G. Ramis, G. Busca, S. Presto, P. Riani, R. Marazza, M. Sisani, F. Marmottini, U. Costantino, Appl. Catal.A: General, 355, 83-93(2009).

[20] A. Bartecki and Dembicka, D. J. of Inorg. and Nuclear Chem.V.29,I.12, 2907-2916(1967).

[21] J. L. Contreras and G. A. Fuentes, Studies in Surface Science and Catalysis, Vol. 101 Edit. B. Delmon and J. T. Yates, Elsevier 1195-1204 (1996).

[22] A. Iannibello, L. Villa, and S. Marengo, Gazzetta Chimica Italiana,109, 521(1979).

[23] M. de los Ángeles Ocaña Z. Síntesis de Hidrotalcitas y Materiales Derivados: Aplicaciones en Catálisis Básica. Tesis de Doctorado, Universidad Complutense de Madrid. (2005).

[24] L. Salvati, L. E. Makovsky, J. M. Stencel, F. R. Brown, D.M. Hercules,J. Phys.Chem.85, 3700-3707(1981).

[25] J. A. Horsley, I. E. Wach, JÑ. M. Brown, G. H. Via, F. D. Hardcastle, J. Phys. Chem.91,15 4014–4020 (1987).

[26] W. P. Griffith and T.D. Wickins, J. Chem.Soc. A. 1087(1966).

[27] J.R. Rostrup-Nielsen, N. Hojlund in: J. Oudar, H. Wise (Eds.), Deactivation and Poisoning of Catalyst, Marcel Dekker, New York, Basel, p.57 (1985).

[28] J. Comas, F. Mariño, M. Laborde, N. Amadeo. Chem Eng. J. 98, 61-68(2004).

[29] A. Erdohelyi, J. Rasko, T. Kecskes, M. Toth, M.Dömök, K.Baán, Catal. Today 116,367-376(2006).

[30] J. L. Contreras, M.A. Ortiz, G. A. Fuentes, R. Luna, J. Salmones, B. Zeifert, L. Nuño and A.Vázquez, J. of New Materials for Electrochemical Systems, 13, 253-259 (2010).

[31] L. Liu, D. Chen, K. Zhang, J. Li, N. Shao, Int. J. of Hydrogen Energy, 33, 3736-3747(2008).

[32] L. J. I. Coleman, W. Epling, R.R. Hudgins, E. Croiset, Appl. Catal., A: General, 363, 52-63(2009).

[33] L. He, H. Berntsen, De Chen, J. of Phys. Chem., A, Vol. 114, 3834-3844(2010).

[34] A. F. Lucrédio, J. D. A.Bellido, E.M. Assaf, Appl. Catal. A: General 388, 77-85(2010).

[35] G. Zeng, Q.Liu, R. Gu, L. Zhang, Y. Li, Catal.Today Volume 178, Issue 1, p. 206-213(2011).

[36] R. Guil-López, R. M. Navarro, M. A. Peña, J. L. G. Fierro, Int. J. of Hydrogen Energy 36, 1512-1523(2011).

[37] J. Llorca, N. Homs, P. Ramírez de la Piscina, J. of Catal. 227, 556-560(2004).